PROCEEDINGS of the
23rd International Congress on Acoustics

9 to 13 September 2019 in Aachen, Germany

CFD modeling of pressure variation in a road cavity with volume variation

Marianne BOU LEBA BASSIL[1]; Julien CESBRON[2]; Philippe KLEIN[3]

[1] IFSTTAR, CEREMA, UMRAE, F-44344 Bouguenais, France

[2] IFSTTAR, CEREMA, UMRAE, F-44344 Bouguenais, France

[3] Univ Lyon, IFSTTAR, CEREMA, UMRAE, F-69675, Lyon, France

ABSTRACT

This paper deals with the variation of air volume at the contact interface between a rolling tyre and a road cavity leading to aerodynamic phenomena such as air-pumping. A numerical model was developed (in 2D and 3D) based on Computational Fluid Dynamics, using the Fluent solver, coupled with a displacement function of the bottom of the cavity representing its volume variation. Results showed that the maximum pressure reached at the bottom of the cavity during its complete closure increased as its volume decreased. The pressure variation was related to the volume variation by a relationship close to Laplace law for perfect gases. In addition, pressure oscillations after the opening of the cavity increased in amplitude and frequency as its volume decreased. Moreover, in the case of the experimental setup of Hamet (1990), introducing the volume variation estimated by Laplace law in the 3D model has shown better agreement between the calculated pressure and the measured pressure in comparison with the model neglecting this volume variation. Future work would therefore be to obtain the actual volume variation caused by the penetration of the tyre tread inside the cavity. This could be done either experimentally or numerically using a tyre/road contact model.

Keywords: Tyre/road noise, Air-pumping, Computational Fluid Dynamics

1. INTRODUCTION

Several generation mechanisms are responsible for tyre/road noise emission. Among these, air-pumping is an aerodynamic source that contributes to rolling noise in the medium and high frequency range. It is usually meant by this term a series of rapid air compression and release at the tyre/road interface and the possible associated resonances.

Air-pumping phenomenon was often attributed to variation of air volumes due to the rubber deformation in the contact patch caused by road asperities indentation (1) or tyre grooves squeezing (2–4). Recent works based on Computational Fluid Dynamics (CFD) have shown that the effect of viscous boundary layer at the tyre and road surfaces also contributes to the generation of pressure fluctuations that are likely to produce noise emission (5,6).

This paper deals with the rather simple geometrical case of a slick tyre rolling on a cylindrical cavity inserted in a smooth road surface. This case was experimentally addressed in Hamet (7,8) and showed a three-phase process: first a gradual air pressure increase in the cavity as the tyre approaches, then a constant overpressure stage during the full cavity closure by the tyre, and finally a pressure release with an Helmholtz resonance when the tyre leaves the cavity. This case was investigated by Conte (5,9) with CFD simulations without considering the tyre rubber penetration in the cavity. Although the mechanism at stake was qualitatively reproduced, there was a significant underestimation of the overpressure inside the cavity compared to experimental results.

In this paper both viscous layer effect and volume variation due to the tyre rubber penetration in the

[1] marianne.bassil@ifsttar.fr
[2] julien.cesbron@ifsttar.fr
[3] philippe.klein@ifsttar.fr

cavity during its closure are considered in CFD simulations. The volume variation is introduced in a simplified manner. Its influence is highlighted regarding the overpressure reached in the cavity. The resulting pressure waves travelling to the front and to the rear of the tyre are compared too.

2. RESULTS OF CFD MODEL WITHOUT VOLUME VARIATION

2.1 Context

Solving fluid dynamics problem usually requires the calculation of various flow properties such as velocity, density, pressure, and temperature as functions of space and time. The equations that govern the motion of a fluid are the Navier-Stokes equations and its derivatives. These are nonlinear differential equations describing the movement of fluids. They are obtained by applying conservation laws such as the conservation of mass (also called the continuity equation), the conservation of momentum (Newton's second law), and the conservation of energy. These equations, when they are not simplified, do not have analytical solution and are therefore only solvable with numerical simulations based on Computational Fluid Dynamics (CFD). The ANSYS Fluent software is based on the finite volume method to solve the Navier-Stokes equations governing the fluid flow. The model chosen for the numerical simulation is the one developed during the work of (5,10) (2D model) and (9) (3D model) simulating the passage of a smooth tyre on a cylindrical cavity. In the case of this air-pumping study, the numerical resolution of the problem enables the calculation of the dynamic pressure of the air at the bottom of the cavity during rolling. The same geometry and mesh were used but some parameters were modified in the method for solving the problem in Fluent.

2.2 CFD model

2.2.1 Configuration

A sketch of the general concept of modeling is represented Figure 1: a slick tyre with a diameter of 631.4 mm rolls on a cylindrical cavity inserted in a smooth road surface with a diameter of 15 mm and a depth of 30 mm at a speed of 22.2 m/s (80 km/h). The chosen parameters enable to compare the results with the measurements reported in Hamet (7) for the same dimensions.

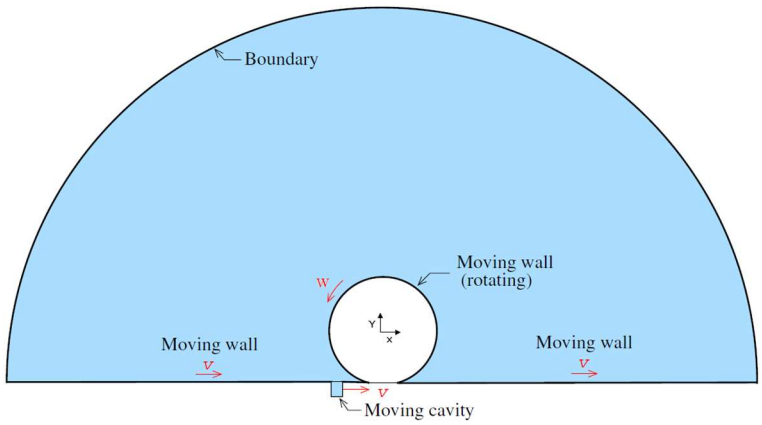

Figure 1 – General concept of the CFD model of a rolling tyre on a cylindrical cavity

Figure 2a shows the 2D geometry of the model and its mesh configuration. The fluid domain around the tyre is formed by a half-disc of 2.5 m radius divided into sub-domains according to their physical importance with respect to the flow: the most critical zones are the regions in front and behind the contact zone and the cavity. These areas are meshed finer than the others. The mesh becomes all the more coarse as one moves away from the contact zone.

The 3D geometry of the model and its mesh configuration are represented in Figure 2b. We consider half the field of computation by introducing a condition of symmetry in the vertical plane cutting the tyre and the cavity in order to reduce the computational cost. The area around the tyre is thus constituted by a quarter sphere of 1 m radius. This sphere is then divided into several subdomains for the same mesh criterion as for the 2D case. The static deformation of the tyre was considered for both 2D and 3D cases. The corresponding contact length is 92 mm in the rolling direction.

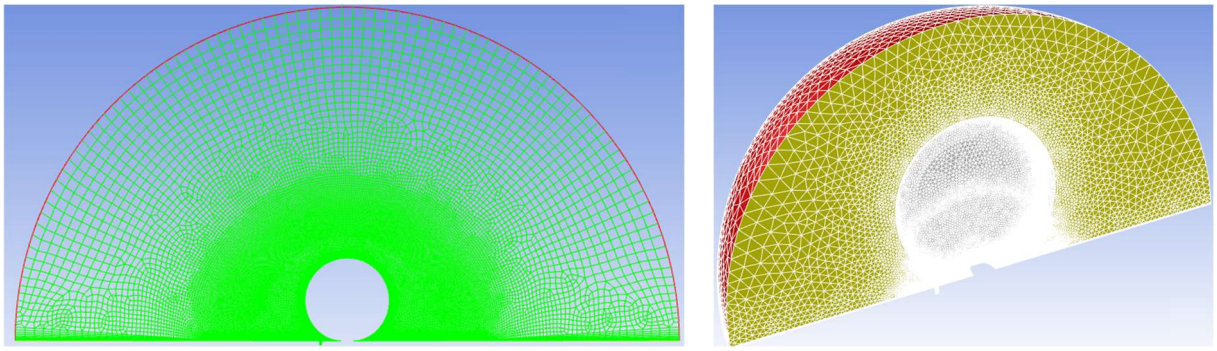

a) b)

Figure 2 – a) 2D meshed geometry; b) 3D meshed geometry

2.2.2 Method of resolution

The reference frame is chosen at the center of the wheel and therefore the tyre is considered to rotate with an angular velocity ω of 71.7 rad/s while the cavity and the roadway are in translational motion with a velocity v of 22.2 m/s. The sliding mesh technique at the cavity/road interface has been adopted. The airflow on the wheel is not considered in this case due to its low contribution to the overpressure generated in the cylindrical cavity and its negligible effect on the main mechanism studied (5). Thus, airflows are generated only by the surface displacement and the development of corresponding boundary layers due to air viscosity.

The boundary limiting the artificially truncated domain leads to reflection of outgoing waves. Non-reflective boundary conditions are imposed at the disk (2D case) or the sphere (3D case) boundary to control spurious wave reflections.

The considered flow is turbulent and controlled by the boundary layer phenomenon. A near-wall treatment is therefore necessary to solve the flow in the inner zone of the boundary layer. The $k-\omega$ SST turbulence model is used to solve the equations, this model being the most appropriate for this type of flow.

Since the flow is unsteady and considered compressible for enabling the evaluation of pressure variations, furthermore a case of rotation, the resolution of the problem is based on the PISO scheme (implicit sequential method). The pressure-based solver is used to solve the problem in two steps. In a first step, the cavity is fixed and the solution of a stationary flow is computed. This latter is used in a second step as the initial condition to solve the unsteady problem with the cavity in translational motion. The cavity being at a distance of 0.2 m before the center of the contact zone, the simulation duration is 0.018 s in order to have the cavity at a symmetrical distance from the beginning of the simulation. The time step is Δt = 2.5e^{-6} s for 2D simulations and 5e^{-6} s for 3D simulations (a coarser spatial resolution is used in 3D).

2.2.3 Results and comparison to experimental results

Figure 3a shows the air pressure calculated in 2D and 3D and Figure 3b shows the measured air pressure at the bottom of the cavity reported in Hamet (7). The average maximum pressure measured is approximately 1740 Pa while those calculated in 2D and 3D are respectively 828 Pa and 969 Pa. The pressure difference ΔP between measured and calculated values is then 912 Pa in 2D and 771 Pa in 3D. This difference can be explained in several ways. Firstly, the airflow around the tyre due to its displacement was estimated by Conte (11) and can produce an overpressure around 200 Pa which is here not taken into account in the simulation. Secondly, the dynamic deformation of the tyre tread and its penetration into the cavity are neglected. In the following, this paper focuses on the last phenomenon. Indeed, the penetration of the tread in the cavity causes a slight reduction in the volume of the cavity, which in turn increases the maximum pressure reached at the bottom of the cavity when it is completely closed. In the next section, the volume variation is introduced in the CFD model (2D and 3D simulations) to evaluate its influence on the variation of the overpressure at the bottom of the cavity.

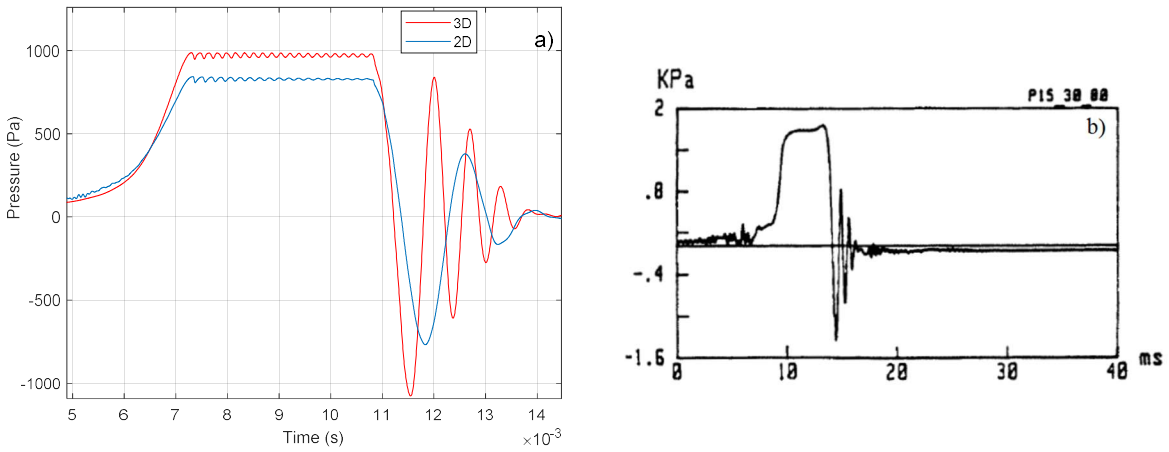

a) b)

Figure 3 – a) Calculated air pressure at the bottom of the cavity; b) Measured air pressure (7)

3. CFD MODEL WITH VOLUME VARIATION

3.1 Calculation of the volume variation

The volume variation is introduced in a simplified way, which is referred as the piston method, by acting on the depth of the cavity (Figure 4). It is thus considered that the bottom of the cavity moves vertically upwards as the cavity closes to reach a maximum value of displacement considered constant during the course of the contact zone (plateau phase) and moves down symmetrically when it opens.

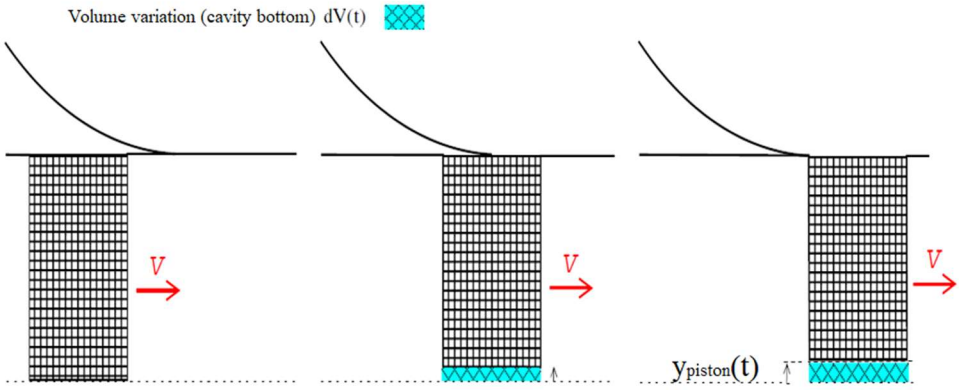

Figure 4 – Sketch of the piston displacement method to describe volume variation

In order to represent the displacement of the bottom of the cavity as a function of time, noted $y_{piston}(t)$, a Tukey window function $w(t)$ (tapered cosine window) is used, which satisfactorily fits the compression, plateau and expansion phases observed in the experimental results. $y_{piston}(t)$ is obtained via the maximum displacement d_i of the cavity bottom and the function $w(t)$ by the following equation:

$$y_{piston}(t) = d_i \; w(t) \tag{1}$$

The mathematical formula of the Tukey function $w(t)$ is as follows:

$$w(t) = \begin{cases} \{1 + \cos(2\pi[t - r/2]/r)\}/2, & 0 \le t < r/2 \\ 1, & r/2 \le t < 1 - r/2 \\ \{1 + \cos(2\pi[t - 1 + r/2]/r)\}/2, & 1 - r/2 \le t < 1 \end{cases} \tag{2}$$

where t is the time vector at N linearly spaced points. The parameter r is the ratio between the length of the tapered cosine section and the total length of the window with $0 \le r \le 1$.

The parametric study is performed in 2D, which is less time-consuming. The displacement of the piston is adapted to the numerical model regarding the time discretization, start time, duration of each phase, etc. as shown in Figure 5. In this case, $r = 0.279$ and $N = 1927$ points.

The percentage of volume decrease $(100\,\Delta V/V_0)$ of the cavity during the compression phase was varied according to the values [0; -0.2; -0.4; -0.6; -0.8; -1; -2; -3; -4; 5; -10; -15; -20; -25] (in %), which corresponds to a maximum displacement of the cavity bottom d_i varying from 0 to 7.5 mm. V_0 is the initial reference volume of the cavity ($\Delta V/V_0 = 0$ and cavity depth L_0= 30 mm).

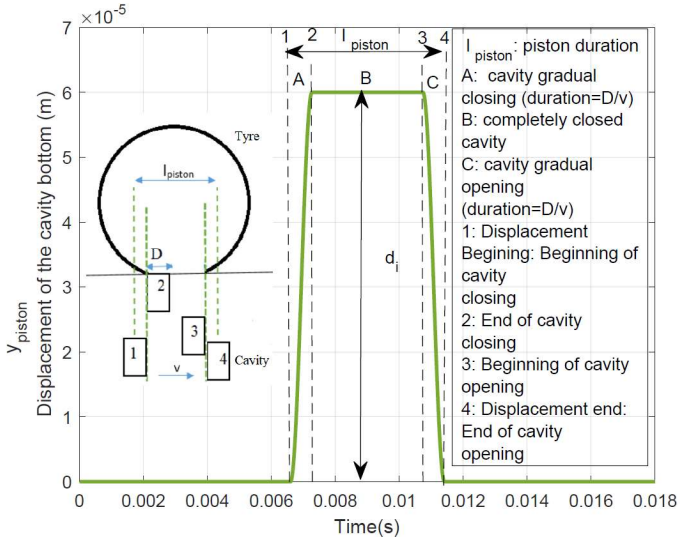

Figure 5 – Displacement of the cavity bottom as a function of time

3.2 Implementation of the volume variation into Fluent

Fluent processes the Dynamic Mesh (DM) together with the sliding motion technique in order to handle the topological changes of the domain during the simulation. There are several methods of dynamic meshing, whose most used are smoothing (this method moves the border and the inner nodes to absorb the movement of the moving border) and layering (used to add or remove cell layers). In the present model, the smoothing method is used for volume variations up to 2 % and the layering method is used for higher volume variations. The dynamic mesh is attributed to the bottom of the cavity considered as the deforming zone.

The displacement function $y_{piston}(t)$, calculated according to Eq. (1), is assigned to the cavity bottom using the UDF (User Defined Function) option in Fluent solver, based on C language. This function describes the movement of the bottom of the cavity by assigning, for each node j of the cavity bottom and each time step, its vertical position y_j according to the following equation:

$$y_j(t) = y_0 - L_0 + y_{piston}\ (t) \tag{3}$$

where $y_0 < 0$ is the vertical position of the road and L_0 is the reference depth of the cavity ($L_0 = 30\ mm$). The average air pressure $p(t)$ is calculated at the bottom of the cavity. For each percentage i of volume variation, p_i is the maximum pressure reached during the contact phase.

3.3 Results

3.3.1 Influence of volume variation

Figure 6 shows the results of the pressure variation as a function of the volume variation with regard to the compression and plateau phases and the expansion phase (pressure oscillations). The maximum pressure reached at the bottom of the cavity during the plateau phase is greater when the cavity volume variation is considered. The higher the volume decreases the higher the overpressure increases. Then, the penetration of the tread causing the volume decrease of the cavity has a significant impact on the overpressure at the bottom of the cavity during the passage of the tyre. The amplitude as well as the frequency of the oscillations of the plateau increase when the volume decreases. In fact, the cavity is acting like a closed tube during this phase leading to the cavity resonance phenomenon characterized by a frequency inversely proportional to the depth of the cavity. Similarly, the amplitude as well as the frequency of the pressure oscillations during the expansion phase increase when the volume decreases.

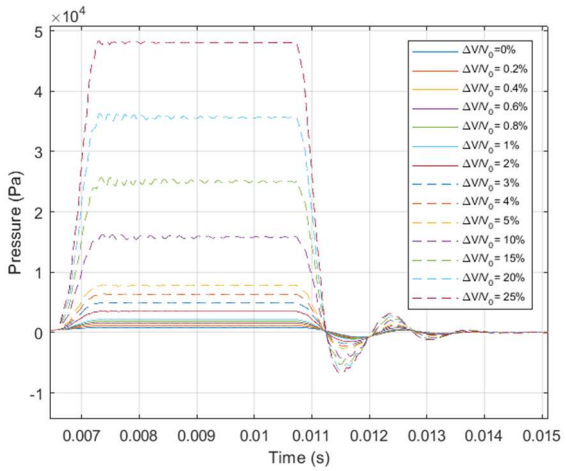

Figure 6 – Influence of the volume variation on the air pressure at the cavity bottom

3.3.2 Relation between the pressure variation and the volume variation

For each percentage of volume variation, the variation of the maximum pressure $\Delta P_{CFD} = p_i - p_0$ is evaluated, with p_0 the reference maximum pressure without volume variation. Figure 7 shows ΔP_{CFD} values as a function of volume variation (lower red curve, "Simulations").

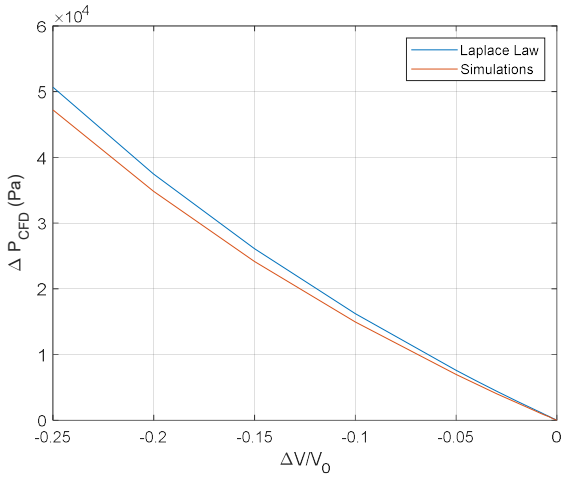

Figure 7 – Variation of the overpressure ΔP with the variation of the cavity volume

This result can be compared to the classical Laplace law in thermodynamics, which gives the relation between the pressure and the volume of a perfect gas undergoing an isentropic transformation:

$$P_i \ V_i^{\gamma} = P_0 \ V_0^{\gamma} \tag{4}$$

where P_i and P_0 are respectively the absolute pressures of the gas after and before the change of volume ($P_i = p_{i,lap} + p_{atm}$, p_{atm} is the atmospheric pressure = 101 325 Pa and $p_{i,lap}$ is the relative pressure of the gas), V_i and V_0 are respectively the volumes of the gas after and before the volume change, and γ =1.4 is the Laplace coefficient. By replacing V_i by $V_i = V_0 (1 + \Delta V/V_0)$ in Eq. (4), the pressure variation ΔP_{Lap} calculated by Laplace law can be written:

$$\Delta P_{Lap} = P_i - P_0 = p_{i,Lap} - p_0 = P_0\left[(1 + \Delta V/V_0)^{-\gamma} - 1\right] \tag{5}$$

The theoretical overpressure ΔP_{Lap} is compared to the ΔP_{CFD} obtained by the 2D simulations in Figure 7 (upper blue curve, "Laplace Law"). The variation of the maximum pressure reached at the bottom of the cavity follows a law which is close to Laplace law (difference between 6.8 % and 8.9 %).

3.3.3 Comparison with measurement

For very small volume variations with respect to the volume of the cavity, Eq. (5) can be linearized as follows:

$$\Delta P_{Lap} = P_0[1 - \gamma \, \Delta V/V_0 - 1] \cong -\gamma P_0 \, \Delta V/V_0 \tag{6}$$

The latter equation can be used to calculate the cavity volume variation from the pressure difference found between the measurements and the CFD model with no volume variation. The volume

variation is then introduced in the CFD model using the piston method described in section (3.2) in order to compute the resulting air pressure at the bottom of the cavity. According to the section (2.2), for the 2D case, the pressure difference ΔP between the measurements and the calculation amounts to 912 Pa. By applying Eq. (6), the volume variation $\Delta V/V_0$ to offset ΔP is estimated to be -0.64%.

This corresponds to a maximum displacement of the cavity bottom equal to 0.192 mm. Figure 8a shows the result of the 2D simulation corresponding to this displacement. A maximum pressure of about 1670 Pa is obtained, which is close to the measured value (4% error compared to the measurements).

The same correction is performed with the 3D geometry for which the dynamic mesh of the piston is modeled by the layering method, most suitable for the 3D mesh of the cylindrical cavity. From the section (2.2), the difference between the measurement and the calculation is 771 Pa. By applying Eq. (6), the corresponding volume variation $\Delta V/V_0$ is -0.54%.

This corresponds to a maximum displacement of the cavity bottom equal to 0.162 mm. Figure 8b shows the result of the 3D simulation corresponding to this displacement. The maximum pressure is about 1605 Pa, which is also close to the measured value (7.7 % error). Furthermore, by comparing the pressure oscillations of the expansion phase with those reported by Hamet (7), a good agreement is found in terms of amplitudes and frequencies. Note that volume variation has a weak influence on the oscillations.

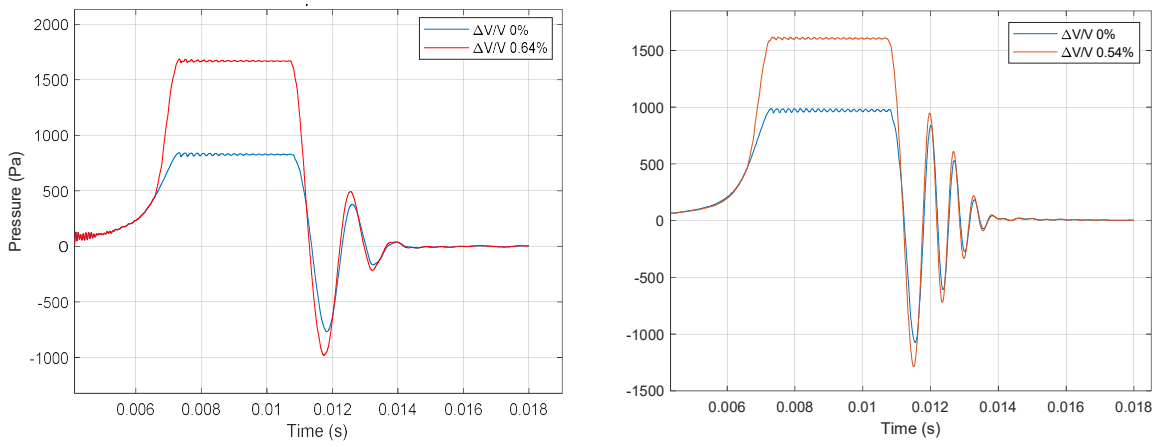

a) b)

Figure 8 – Results of the CFD model with volume variation a) 2D; b) 3D

On the other hand, Figure 9a and Figure 9b show the 3D air pressures calculated respectively at the leading and the trailing edges (located at 20 cm on both sides of the contact zone), compared to the case without volume variation. There is a decrease in amplitude of the pressure wave generated at the leading edge (more pronounced at the minimum of pressure than at the maximum), with the decrease of volume. On the other hand, the amplitude of the oscillations at the trailing edge slightly increases (by 17% approximately) with the decrease of volume.

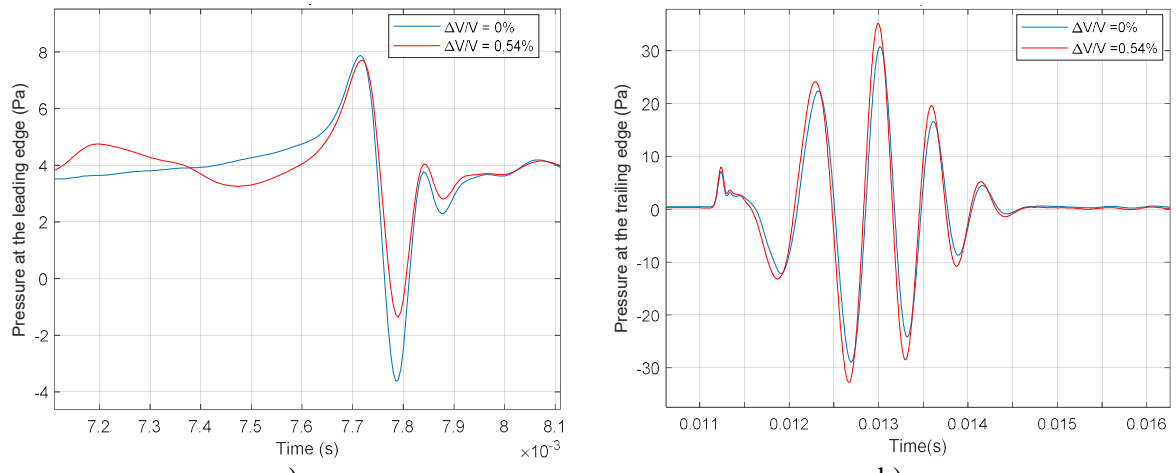

a) b)

Figure 9 – Pressure calculated in 3D: a) at the leading edge and b) at the trailing edge

4. CONCLUSIONS

This paper highlights the influence of the volume variation of the cavity on the dynamic pressure of the air at the tyre/road interface during the rolling of a smooth tyre on a cylindrical cavity incorporated in the pavement. The variation of volume has been introduced in a simplified piston method by considering that the bottom of the cavity moves vertically upward as the cavity closes to reach a maximum value of displacement considered constant during the course of the contact. Then, the bottom of the cavity moves down symmetrically when it opens.

A 2D calculation with the commercial code ANSYS Fluent allowed to make a parametric study and to deduce a relation between the variation of the maximum pressure reached at the bottom of the cavity and the variation of volume of the latter during the contact. The overpressure generated during the contact increases with the decrease of the volume of the cavity according to a relation close to Laplace's law indicating an isentropic transformation (reversible and adiabatic). These data were then used for the comparison between the simulations of a smooth tyre running on a cylindrical cavity and the experimental results of (7) using the same parameters. The calculations are close to the measurements when the volume variation of the cavity is introduced into the numerical model. For this particular case of a fully closed cavity, although the rubber penetration strongly influences the pressure in the cavity, it seems to have little effect on the noise generated.

The volume variation has been estimated based on Laplace law and an approximate function. It would therefore be interesting to find the exact volume variation of the cavity instead of estimating it. This could be done by using two methods. The first one could be a numerical method using a tyre/pavement contact model for calculating the penetration of the tread into the cavity during the rolling and thus deducing the resulting volume variation. The second one could be an experimental method, which consists of measuring the penetration of the tyre tread by specific displacement sensors.

ACKNOWLEDGEMENTS

This work has been jointly funded by the French Region of Pays de la Loire and IFSTTAR.

REFERENCES

1. Ronneberger D. Towards a quantitative prediction of tire/road noise. Proc Workshop on Rolling Noise Generation; Berlin, Germany 1989. p. 218-234.
2. Ejsmont JA, Sandberg U, Taryma S. Influence of tread pattern on tire/road noise. SAE International Reports. 1984;841238:5632-5640.
3. Hayden RE. Roadside noise from the interaction of a rolling tire with the road Surface. J Acoust Soc Am. 1971;50(1A):113-113.
4. Kim S, Jeong W, Park Y, Lee S. Prediction method for tire air-pumping noise using a hybrid technique. J Acoust Soc Am. 2006;119(6):3799-3812.
5. Conte F, Philippe J. CFD modelling of air compression and release in road cavities during tyre/road interaction. Proc. Euronoise 2006; 30 may - 1 June 2006; Tampere, Finland, 2006.
6. Pinnington RJ. A compressible fluid model for opening and closing dynamics. ITARI project Deliverable 2.1b, 2007.
7. Hamet JF, Deffayet C, Pallas MA. Phénomènes d'air-pumping dans le bruit de contact pneumatique/chaussée. Cas d'une cavité aménagée dans la chaussée. Rapport INRETS N°132;1990.
8. Hamet JF, Deffayet C, Pallas MA. Air-pumping phenomena in road cavities. Proc International Tire/Road Noise Conference; August 1990; Gothenburg, Sweden; 1990. p. 29-35.
9. Conte F, Klein P. 3D CFD modelling of air pumping noise from road cavities with constant volume. Proc Internoise 2013; 15-18 September 2013; Innsbrück, Austria 2013.
10. Conte F, Klein P, Berengier M. Investigating lateral porosity effect on air pumping noise from connected road cavities with CFD simulations. Proc Internoise 2014; 16-19 November 2014; Melbourne, Australia 2014.
11. Conte F. Modélisation CFD du phénomène acoustique de pompage d'air dans un contact pneumatique/chaussée. PhD Thesis. INSA de Lyon; 2008.